Acta Crystallographica Section B
Structural Science
ISSN 0108-7681

Polymorphism of Li_2Zn_3

Volodymyr Pavlyuk,[a,b]* Ihor Chumak[c] and Helmut Ehrenberg[c,d]

[a]Department of Inorganic Chemistry, Ivan Franko National University, Kyryla and Mefodiya str., 6, 79005 Lviv, Ukraine, [b]Institute of Chemistry, Environment Protection and Biotechnology, Jan Dlugosz University, al. Armii Krajowej 13/15, 42-200 Czestochowa, Poland, [c]IFW Dresden, Helmholtzstrasse 20, D-01069 Dresden, Germany, and [d]Karlsruhe Institute of Technology (KIT), Institute for Applied Materials (IAM), Hermann-von-Helmholtz-Platz 1, D-76344 Eggenstein-Leopoldshafen, Germany

Correspondence e-mail: vpavlyuk2002@yahoo.com

Received 28 September 2011
Accepted 12 December 2011

Crystal structures of low- and high-temperature modifications of the binary phase Li_2Zn_3 were determined by single-crystal X-ray diffraction techniques. The low-temperature modification is a disordered variant of Li_5Sn_2, space group $R\bar{3}m$ (No. 166). The high-temperature modification crystallizes as an *anti*-type to Li_5Ga_4, space group $P\bar{3}m1$ (No. 164). Two polymorphs can be described as derivative structures to binary Li_5Ga_4, Li_5Sn_2, $Li_{13}Sn_5$, Li_8Pb_3, $CeCd_2$ and CdI_2 phases which belong to class 2 with the parent W-type in Krypyakevich's classification. All atoms in both polymorphs are coordinated by rhombic dodecahedra (coordination number CN = 14) like atoms in related structures. The $Li_2Zn_{2.76}$ (for the low-temperature phase) and $Li_2Zn_{2.82}$ (for the high-temperature phase) compositions were obtained after structure refinements. According to electronic structure calculations using the tight-binding–linear muffin-tin orbital–atomic spheres approximations (TB–LMTO–ASA) method, strong covalent Sn—Sn and Ga—Ga interactions were established in Li_5Sn_2 and Li_5Ga_4, but no similar Zn—Zn interactions were observed in Li_2Zn_3.

1. Introduction

According to the much published data on the binary Li–Zn system, which have been summarized by Pelton (1991), five compounds are confirmed by X-ray analysis at room temperature. Recently, intermetallic compounds containing lithium, zinc and other metallic or non-metallic elements have been of particular interest to researchers in relation to their useful properties as modern lightweight alloys and anode materials for lithium batteries (Dmytriv *et al.*, 2007; Chumak *et al.*, 2010). It should be noted that the crystal structures of most binary phases have not been well defined yet, although studies have been under way for a long time. Full structural studies have only been carried out for the LiZn phase, which crystallizes in the NaTl structure type (Zintl & Schneider, 1935), and $LiZn_{13}$ belonging to the $NaZn_{13}$ structure type (Fischer & Jansen, 2010). The last phase has not been previously reflected in the diagram, probably because this phase exists at low temperatures and decomposes above room temperature. With the zinc content increasing in Li–Zn alloys, the formation of a binary phase with the approximate composition Li_2Zn_3 (Grube & Vosskühler, 1933) was observed, and a phase transition was obtained at 443 K. Polymorphic transformations are found in other binary intermetallic compounds with lithium, as recently observed for LiAg (Pavlyuk *et al.*, 2010).

The results of crystallographic studies of both the low and high-tempreature modifications of Li_2Zn_3 are reported here.

Table 1
Experimental details.

Experiments were carried out at 296 K with Mo $K\alpha$ radiation using a Bruker Kappa APEXII CCD area-detector diffractometer. Absorption was corrected for by multi-scan methods (*SADABS*; Bruker, 2004*c*). Refinement was with 0 restraints.

	Low-temperature Li_2Zn_3	High-temperature Li_2Zn_3-HT
Crystal data		
Chemical formula	$Li_{0.63}Zn_{0.87}$	$Li_{0.62}Zn_{0.87}$
M_r	61.46	61.87
Crystal system, space group	Trigonal, $R\bar{3}m$	Trigonal, $P\bar{3}m1$
a, c (Å)	4.386 (4), 18.738 (18)	4.3528 (14), 8.003 (3)
V (Å^3)	312.2 (7)	131.31 (8)
Z	14	6
μ (mm^{-1})	22.96	23.57
Crystal size (mm)	0.06 × 0.05 × 0.02	0.07 × 0.06 × 0.02
Data collection		
T_{min}, T_{max}	0.246, 0.609	0.211, 0.623
No of measured, independent, observed [$I > 2\sigma(I)$] reflections	922, 162, 111	1795, 159, 118
R_{int}	0.059	0.156
Refinement		
$R[F > 2\sigma(F)]$, $wR(F^2)$, S	0.028, 0.076, 1.17	0.058, 0.142, 1.27
No. of reflections	162	159
No. of parameters	16	19
$\Delta\rho_{max}$, $\Delta\rho_{min}$ (e Å^{-3})	1.12, −0.82	1.86, −1.08

Computer programs used: *APEX*2 (Bruker, 2004*a*), *SAINT* (Bruker, 2004*b*), *SHELXTL* (Sheldrick, 2008), *DIAMOND* (Brandenburg, 2006), *publCIF* (Westrip, 2010).

2. Experimental

2.1. Synthesis and phase analysis

The Li_2Zn_3 alloy was prepared from lithium rods (99.9%, Alfa Aesar, Karlsruhe, Germany) and zinc shot (99.99%, Alfa Aesar). This alloy is very sensitive to air atmosphere. To avoid oxidation and contamination all preparation steps were performed in a glove box under a controlled argon atmosphere. Calculated amounts of the elements were enclosed in a Ta crucible sealed under an argon atmosphere by arc-welding. The Ta crucibles were heated to 1173 K in an induction oven, held at this temperature for about 10 min before cooling down to room temperature under ambient conditions after switching off the heater. Three different temperatures, 373, 423 and 573 K, were used for annealing the synthesized sample. After each stage of annealing the X-ray phase analysis was carried out. The tabular shaped single crystals, exhibiting metallic luster, were isolated by mechanical fragmentation from the prepared alloy after annealing at 423 and 573 K (referred to as low- and high-temprature phases hereinafter). Differential thermal analysis (DTA) was used for the determination of the phase transition temperature. Differential scanning calorimetry (DSC) measurements were performed using a Netzsch apparatus (DSC 204 HP Phoenix, heat-flow apparatus), which was placed inside a dedicated glove box under Ar. The heating rate was 5 K min^{-1}.

2.2. X-ray crystallography

Appropriate single crystals for X-ray diffraction were selected using a light microscope. Samples were kept under dried paraffin to protect measures against humidity. Crystals were sealed in 0.2 mm capillaries. Single-crystal data collection was performed at 296 K using a Bruker Kappa diffractometer equipped with an Mo tube and CCD APEXII detector. Absorption correction was made using the multi-scan method (*SADABS*; Bruker, 2004*c*). Other single-crystal experimental details are given in Table 1.[1] Crystal structures of low- and high-temperature modifications of Li_2Zn_3 were solved by direct methods in centrosymmetric space groups $R\bar{3}m$ (No. 166) and $P\bar{3}m1$ (No. 164). In low-temperature Li_2Zn_3 all the crystallographic positions are fully occupied by statistical mixtures of the Li and Zn atoms. In high-temperature Li_2Zn_3 the 1*a* and 2*d* crystallographic Wyckoff sites are fully occupied by Zn1 and Zn2, while two 2*d* and one 2*c* sites are occupied by statistical mixtures of Li and Zn atoms. In the final refinement cycles all atoms were successfully refined with anisotropic displacement parameters. The atomic coordinates were standardized using the *STRUCTURE TIDY* program (Gelato & Parthé, 1987). The crystal structure and phase purity were also confirmed by X-ray powder diffraction using a Stoe Stadi/P powder diffractometer (Co $K\alpha_1$ radiation).

2.3. Electronic structure calculations

The linear muffin-tin orbital (LMTO) method (Andersen, 1975, 1984; Skriver, 1984) in its tight-binding representation (Andersen & Jepsen, 1984), which corresponds to a fast linearized form of the Korringa–Kohn–Rostoker (KKR) method (Korringa, 1947; Kohn & Rostoker, 1954), was used for electronic structure calculations on low- and high-temperature Li_2Zn_3, Li_5Ga_4 and Li_5Sn_2. The calculations were made using basic sets composed of short-ranged atom-centered TB–LMTOs without empty spheres. The *TB-LMTO-ASA* 4.7 program was taken for the calculations with a scalar-relativistic Hamiltonian and atomic spheres approximations (Krier *et al.*, 1995). Electronic energies were calculated *via* density-functional theory (DFT) based on the local-density approximation (LDA) for the exchange-correlation functional, as parametrized by von Barth & Hedin (1972). Diagonalization and integration in reciprocal space were performed using an improved tetrahedron method (Blöchl *et al.*, 1994). In order to evaluate various orbital interactions, the density of states (DOS), the crystal orbital Hamilton popula-

[1] Supplementary data for this paper are available from the IUCr electronic archives (Reference: BP5039). Services for accessing these data are described at the back of the journal.

tion (COHP) curves (Dronskowski & Blöchl, 1993) and the integrated COHP values (iCOHPs) were also calculated. A mapping of the electrons within real space was obtained from the calculations using the electron-localization function (ELF; Becke & Edgecombe, 1994).

3. Results and discussion

Binary alloys were prepared within the Li–Zn system for the concentration region with a high content of zinc (from 50 to 95 at.% Zn) in the course of the systematic studies. The existence of the earlier reported Li_2Zn_3 binary compound has been confirmed. X-ray powder diffraction and differential thermal analyses of this alloy also confirmed a phase transition at 438 K (Fig. 1). As the crystal structures of both modifications remained unknown, these phases were further investigated by single-crystal X-ray diffraction. The single-crystal data show that the low-temperature modification has trigonal symmetry as a strongly disordered variant of the Li_5Sn_2 structure type (space group $R\bar{3}m$). The Li_5Sn_2 type is a fully ordered structure where one crystallographic 6*c* site is occupied by Sn atoms, and two other 6*c* sites and one *3a* site are occupied by Li atoms. In contrast, all these sites are occupied by a statistical mixture of Zn and Li atoms in the low-temperature Li_2Zn_3 structure. The crystal structure of the high-temperature modification can be described as an *anti*-type of Li_5Ga_4 (space group $P\bar{3}m1$), because the Li sites in Li_5Ga_4 are occupied by Zn in high-temperature Li_2Zn_3, while the Ga sites in Li_5Ga_4 are occupied by a statistical mixture of lithium and zinc. When occupation parameters have been refined, the compositions of the polymorphs are determined as $Li_2Zn_{2.76}$ (for the low-temperature phase) and $Li_2Zn_{2.82}$ (high-temperature phase) or $Li_{42}Zn_{58}$ and $Li_{41}Zn_{59}$ in at.%. It is very close to the starting composition $Li_{40}Zn_{60}$ (or Li_2Zn_3).

According to X-ray phase analysis, which was carried out after annealing at 373 and 423 K, the corresponding alloys were determined as single low-temperature phases with nearly equal unit-cell values: a = 4.38089 (5), c = 18.6547 (2) Å and a = 4.37554 (3), c = 18.6460 (1) Å. After annealing at 573 K the alloy was also single but the high-temperature phase with the unit-cell dimensions: a = 4.34997 (3), c = 8.03799 (7) Å. There is a good agreement between those and powder unit-cell values for both polymorphs: 4.386 (4), 18.738 (18) Å for the low-temperature phase and 4.3528 (14), 8.003 (3) Å for the high-temperature phase.

Unit-cell projections and atomic coordination polyhedra are shown in Fig. 2 for both polymorphs. All these polyhedra are rhombic dodecahedra with the coordination number CN equal to 14. This suggests that both structures belong to class 2 in the classification scheme suggested by Krypyakevich (1977), in which the parent structure belongs to a W-type. Stacking

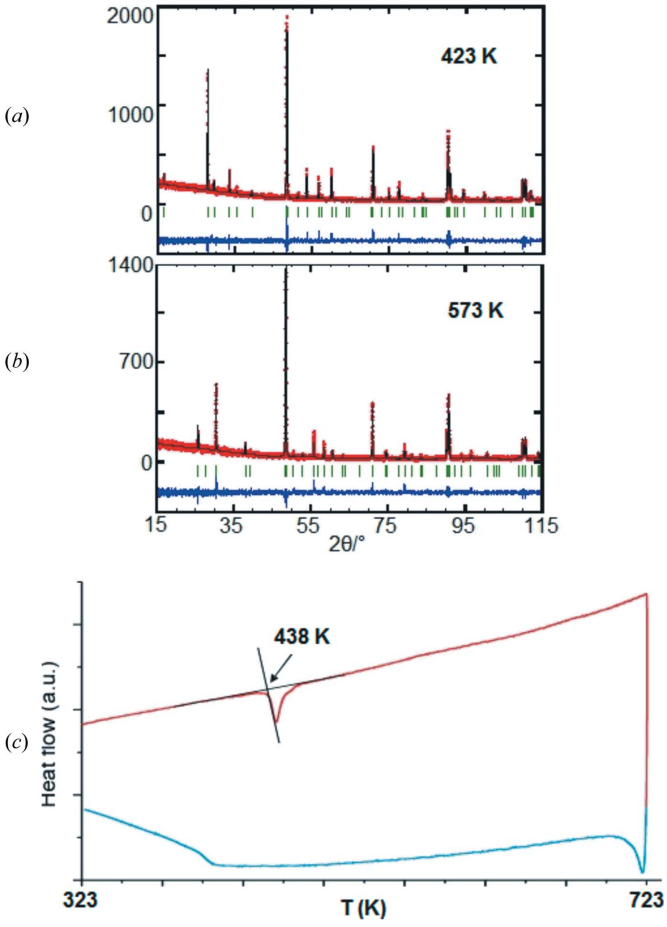

Figure 1
X-ray powder diffraction patterns at (*a*) 423 K amd (*b*) 573 K, and (*c*) DSC curves for the Li_2Zn_3 alloy.

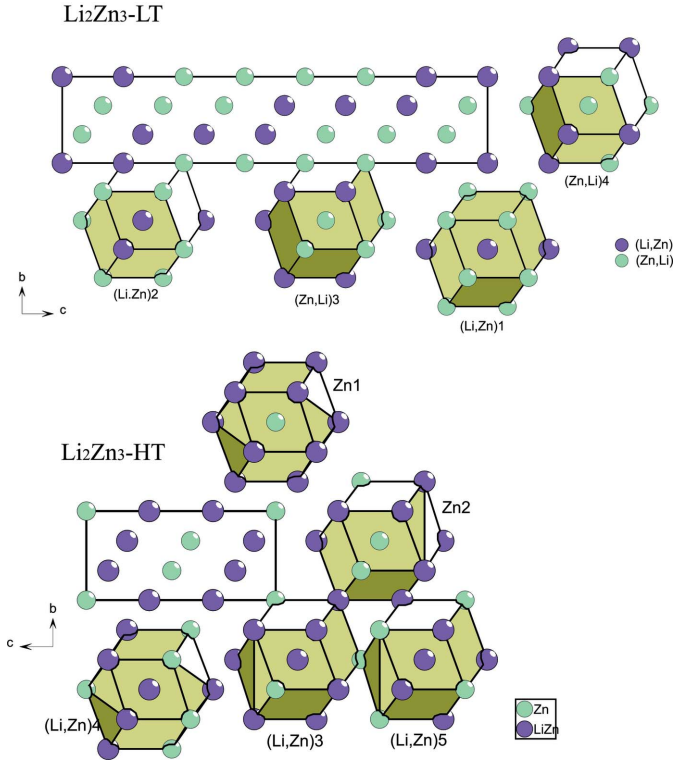

Figure 2
Structure projections and coordination polyhedra in the low- and high-temperature Li_2Zn_3 unit cells.

rhombic dodecahedra in low- and high-temperature Li_2Zn_3 are presented in Fig. 3 compared with those in the W structure. The equality of coordination numbers of each type of atom indicates their similar effective radii, which rate these structures as derivatives of close-packed ones. The shortest interatomic distances indicate metallic bonds typical of intermetallic compounds.

Alternatively, the structures of both Li_2Zn_3 polymorphs can be described as combinations of simple ordered and disordered fragments of the trigonal $CeCd_2$ structure type (Iandelli & Ferro, 1954) and its CdI_2 *anti*-type (Bozorth, 1922; Fig. 4). The structures of other compounds within the binary systems of lithium with a group III–IV *p*-element, such as Li_5Ga_4, Li_5Sn_2, $Li_{13}Sn_5$ (Frank & Müller, 1975) and Li_8Pb_3 (Cenzual *et al.*, 1990) are composed of the same fragments. Note that similar structures are also realised in lithium-containing ternary systems if the third component is a transition metal, such as $Li_5Cu_2Ge_2$ (Pavlyuk & Bodak, 1992), which is an ordered superstructure of Li_5Ga_4, and $Li_9V_4Sn_5$, which is an ordered superstructure of $Li_{13}Sn_5$ (Azarska & Pavlyuk, 2003*a*,*b*).

The low- and high-temperature polymorphs and their derivative structures, such as Li_5Ga_4, Li_5Sn_2, $Li_{13}Sn_5$, Li_8Pb_3, $CeCd_2$ and CdI_2 (Fig. 4), consist of the structural building units which can be received from the W-type by two mechanisms, such as substitution and deformation. The difference between structural units (marked in Fig. 4 as *A*, *B* and *C* for type and A, B, C and D for *anti*-type) is only in the rate of their ordering. Thus all the described structures differ from each other only in the mutual location of these fragments in the unit cells, especially along the *z* axes, causing their crystallization in different space groups with different values of the cell parameter *c*.

The phase transition of Li_2Zn_3 is driven by an order–disorder process. In the fully disordered structure of the low-temperature polymorph all four crystallographic Wyckoff sites are occupied by statistical mixtures of Li and Zn atoms. While the high-temperature phase exists at temperatures above 438 K, the ordering of the crystal structure is observed. This is also shown by the fact that 40% of crystallographic Wyckoff sites (two among five) are fully occupied by the Zn atoms. The building unit, which is marked 'A' (Fig. 4), stays intact in both polymorphs at the phase transition, while an atomic rearrangement is obtained in other building units, such as '*B*' and 'D' (in the low-temperature phase), and 'C' (in the high-temperature phase).

Electronic structure calculations were performed to analyze chemical bonding in this family of intermetallic compounds in more detail. TB–LMTO–ASA calculations were performed on ordered models, although statistical mixtures of Zn and Li were observed in the real crystal structures for both polymorphs. In simplified calculating models the crystal structures were approximated in such a way that the dominant atomic element was assigned to occupy the site fully, while the minor occupation of the same site by another element was ignored. The electron localization function (ELF) maps for low- and high-temperature Li_2Zn_3, Li_5Ga_4 and Li_5Sn_2 are shown in Fig. 5. Higher electron density (red regions) within the crystal space is observed in the Li_5Sn_2 structure around the Sn atoms, and a significant electron density (ELF > 0.80) is also localized between Ga atoms in Li_5Ga_4. In contrast, no significant concentration of electron density is observed around atoms in both polymorphic modifications of Li_2Zn_3. The corresponding crystal space is marked as a green region (ELF > 0.35–0.45) indicating electron delocalization and free-electron-like behavior. In the case of other ordered models (sorts of atoms in the sites were changed) the similar electron density distribution was observed as well as the absence of strong interactions. This fact and the similarity of the effective radii of Li and Zn atoms are in good agreement with the observed

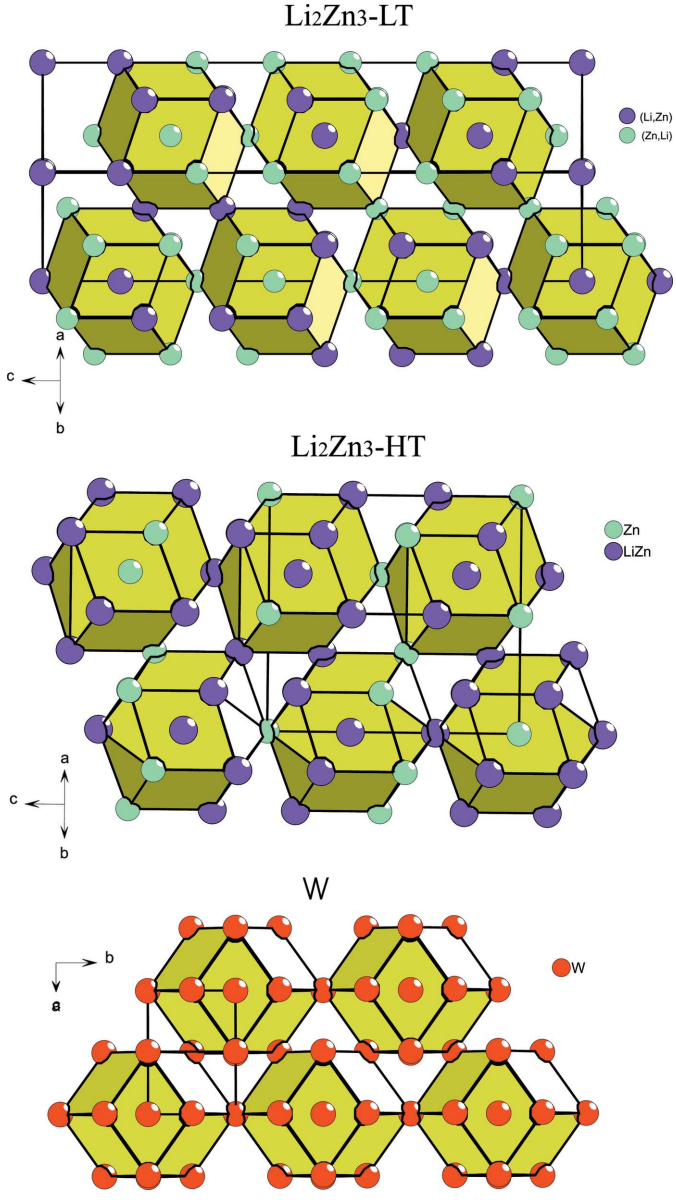

Figure 3
Stacking rhombic dodecahedra in the low- and high-temperature Li_2Zn_3 and parent W structures.

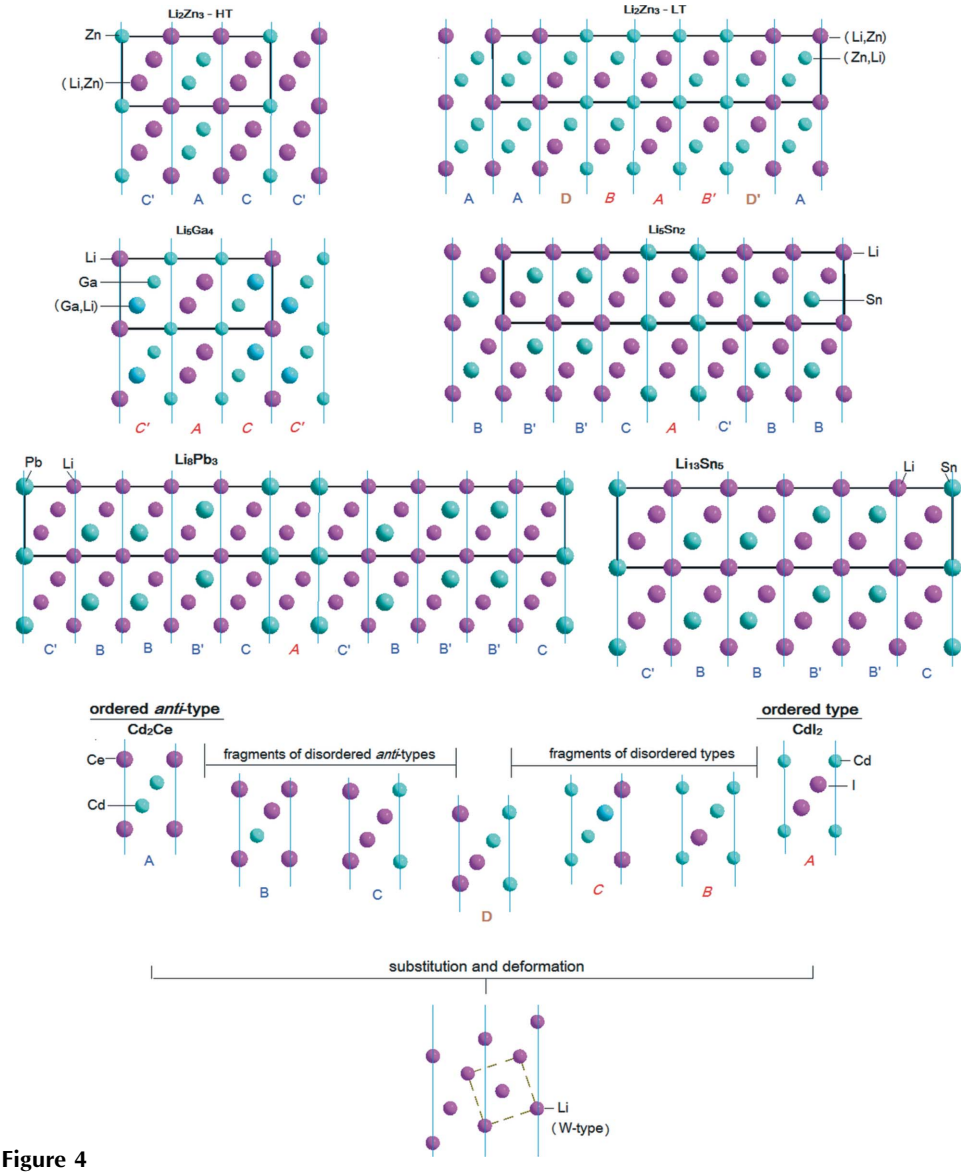

Figure 4
Scheme of the relationship between the low- and high-temperature Li_2Zn_3, Li_5Ga_4, Li_5Sn_2, $Li_{13}Sn_5$, Li_8Pb_3, $CeCd_2$ and CdI_2, and parent W structures.

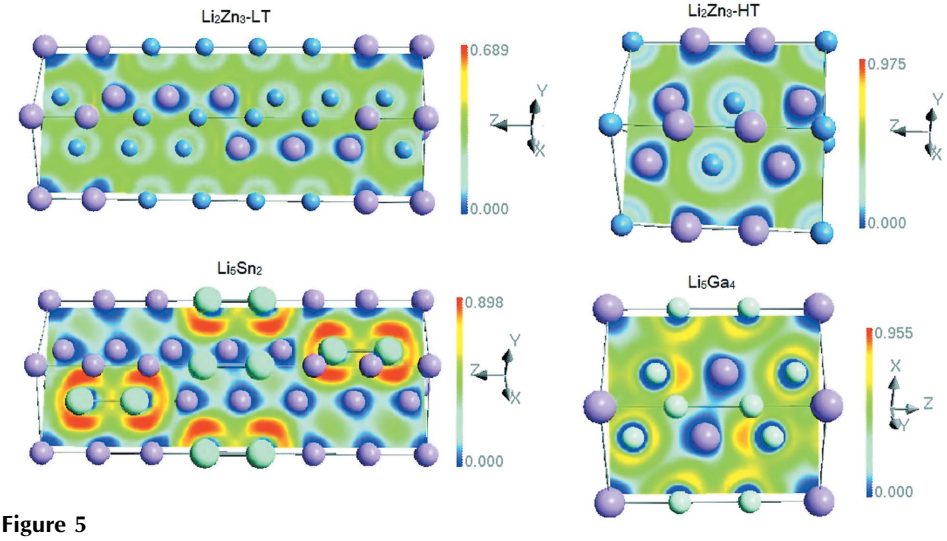

Figure 5
Electron localization function (ELF) maps for low- and high-temperature Li_2Zn_3, Li_5Ga_4 and Li_5Sn_2.

statistical mixture of these atoms at the same crystallographic sites.

The electronic densities of states (DOS) for low- and high-temperature Li_2Zn_3, Li_5Ga_4 and Li_5Sn_2 are presented in Fig. 6. The DOS of these alloys in the region from 0 to more than −9 eV are dominated by contributions from the Zn atoms in cases of both Li_2Zn_3 polymorphs or contributions from the Sn and Ga (in the cases of Li_5Sn_2 and Li_5Ga_4 compounds). The *s*-type states (4*s*-Zn, 4*s*-Ga and 5*s*-Sn) are mainly close to the lower valence band (from −9 to < −6.5 eV) and *p*-type states (4*p*-Zn, 4*p*-Ga and 5*p*-Sn) are located almost in the upper valence band (from −5 to 0 eV).

The chemical bonding exhibits strongly attractive Sn—Sn interactions (integrated crystal orbital Hamilton populations, -*i*COHP = 2.0784 eV per bond per cell) for Li_5Sn_2; Ga—Ga interactions are slightly weaker (-*i*COHP = 1.5973 eV) for Li_5Ga_4, and Zn—Zn interactions are much weaker in both polymorphs: -*i*COHP = 0.7384 eV for low-temperature Li_2Zn_3 and -*i*COHP = 0.6215 eV for high-temperature Li_2Zn_3. The chemical bonding of lithium with zinc and *p*-elements (Sn or Ga) differs slightly, for example -*i*COHP = 0.4312 eV for Li—Zn interactions and -*i*COHP = 0.4500 eV for Li—Sn interactions. These data indicate strong covalent interactions between Sn—Sn or Ga—Ga in Li_5Sn_2 and Li_5Ga_4 but not between Zn—Zn in Li_2Zn_3. The absence of strong interatomic interactions in Li_2Zn_3 is the main reason for phase transitions with small energy expenses, so the phase-transition temperature from low-tempertaure Li_2Zn_3 to high-temperature Li_2Zn_3 is not high (only 438 K).

4. Conclusions

The crystal structures of two Li_2Zn_3 polymorphic modifications

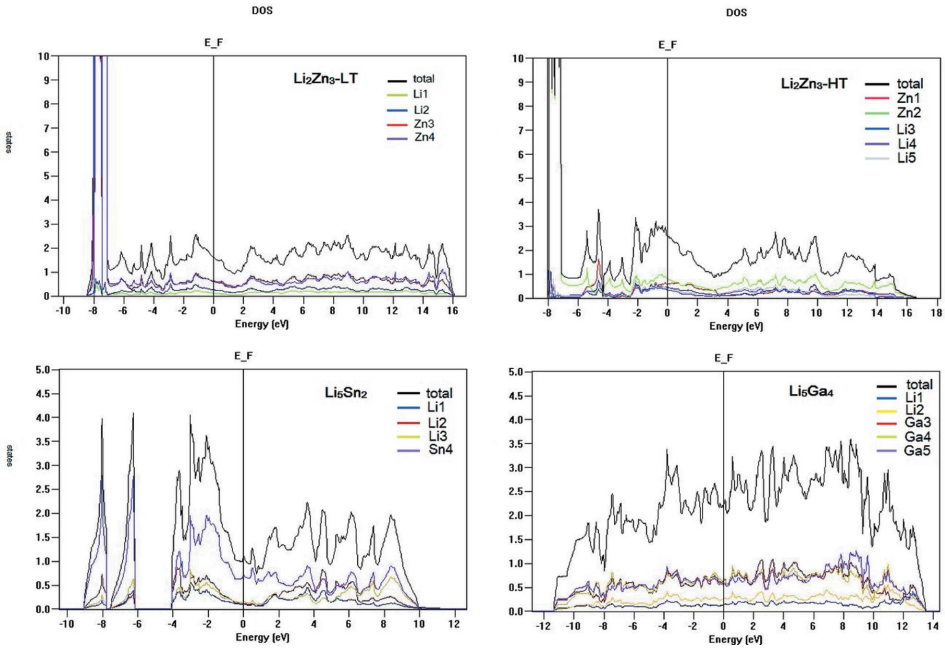

Figure 6
Total and partial DOS for low- and high-temperature Li_2Zn_3, Li_5Ga_4 and Li_5Sn_2.

were determined using X-ray diffraction and thermal analyses. The phase transition temperature was specified as 438 K. The low-temperature modification is a strongly disordered variant of the Li_5Sn_2 structure type and the high-temperature modification crystallizes as the *anti*-type to the Li_5Ga_4 structure. The coordination polyhedra for all atoms are rhombic dodecahedra in both polymorphs. These two polymorphs can be described as derivative structures of binary Li_5Ga_4, Li_5Sn_2, $Li_{13}Sn_5$, Li_8Pb_3, $CeCd_2$ and CdI_2 phases belonging to class 2 in the classification scheme suggested by Krypyakevich, where the parent structure belongs to the W type. We also used data obtained from electronic structure calculations by the TB–LMTO–ASA method in order to evaluate and characterize chemical bonding.

The authors are grateful to Inge Lindemann for carrying out the thermal analysis of the alloy. This work has been supported by the Deutsche Forschungsgemeinschaft (DFG, EH183/7) and the Ministry of Education and Science of Ukraine (M/206-2009), and the Bundesministerium für Bildung und Forschung (BMBF) is gratefully acknowledged.

References

Andersen, O. K. (1975). *Phys. Rev. B*, **12**, 3060–3083.
Andersen, O. K. (1984). *The Electronic Structure of Complex Systems*, edited by P. Phariseau & M. Temmerman. NewYork: Plenum Press.
Andersen, O. K. & Jepsen, O. (1984). *Phys. Rev. Lett.* **53**, 2571–2574.
Azarska, O. & Pavlyuk, V. (2003*a*). *J. Alloys Compd*, **361**, 125–129.
Azarska, O. & Pavlyuk, V. (2003*b*). *Pol. J. Chem.* **77**, 1027–1031.
Barth, U. von & Hedin, L. (1972). *J. Phys. C*, **5**, 1629–1642.
Becke, A. D. & Edgecombe, K. E. (1994). *Nature*, **371**, 683–686.
Blöchl, P. E., Jepsen, O. & Andersen, O. K. (1994). *Phys. Rev. B*, **49**, 16223–16233.
Bozorth, R. M. (1922). *J. Am. Chem. Soc.* **44**, 2232–2236.
Brandenburg, K. (2006). *DIAMOND*, Version 3.1e. Crystal Impact GbR, Bonn, Germany.
Bruker (2004*a*). *APEX*2. Bruker AXS Inc., Madison, Wisconsin, USA.
Bruker (2004*b*). *SAINT*. Bruker AXS Inc., Madison, Wisconsin, USA.
Bruker (2004*c*). *SADABS*. Bruker AXS Inc., Madison, Wisconsin, USA.
Cenzual, K., Gelato, L. M., Penzo, M. & Parthé, E. (1990). *Z. Kristallogr.* **193**, 217–242.
Chumak, I., Dmytriv, G., Pavlyuk, V., Oswald, S., Eckert, J., Trill, H., Eckert, H., Pauly, H. & Ehrenberg, H. (2010). *J. Mater. Res.* **25/8**, 1492–1499.
Dmytriv, G., Pavlyuk, V., Tarasiuk, I., Pauly, H., Ehrenberg, H., Marciniak, B., Prochwicz, W. & Schroeder, G. (2007). *Visn. Lviv. Univ. Ser. Khim.* **48**, 172–178.
Dronskowski, R. & Blöchl, P. E. (1993). *J. Phys. Chem.* **97**, 8617–8624.
Fischer, D. & Jansen, M. (2010). *Z. Anorg. Allg. Chem.* **636**, 1917–1919.
Frank, U. & Müller, W. (1975). *Z. Naturforsch. B*, **30**, 316–322.
Gelato, L. M. & Parthé, E. (1987). *J. Appl. Cryst.* **20**, 139–143.
Grube, G. & Vosskühler, H. (1933). *Z. Anorg. Allg. Chem.* **215**, 211–224.
Iandelli, A. & Ferro, R. (1954). *Gazz. Chim. Ital.* **84**, 463–478.
Kohn, W. & Rostoker, N. (1954). *Phys. Rev.* **94**, 1111–1120.
Korringa, J. (1947). *Physcia*, **13**, 392–400.
Krier, G., Jepsen, O., Burkhardt, A. & Andersen, O. K. (1995). *TB-LMTOASA*, Version 4.7. Max-Planck-Institut für Festkörperforschung, Stuttgart, Germany.
Krypyakevich, P. I. (1977). *Structure Types of Intermetallic Compounds.* Moscow: Nauka. (In Russian).
Pavlyuk, V. & Bodak, O. (1992). *Kristallografia*, **37**, 1027–1030.
Pavlyuk, V., Dmytriv, G., Tarasiuk, I., Chumak, I., Pauly, H. & Ehrenberg, H. (2010). *Solid State Sci.* **12**, 274–280.
Pelton, A. D. (1991). *J. Phase Equilib.* **12**, 42–45.
Sheldrick, G. M. (2008). *Acta Cryst.* A**64**, 112–122.
Skriver, H. (1984). *The LMTO Method.* Berlin: Springer-Verlag.
Westrip, S. P. (2010). *J. Appl. Cryst.* **43**, 920–925.
Zintl, E. & Schneider, A. (1935). *Z. Elektrochem. Angew. Phys. Chem.* **41**, 764–767.